Table 1. Incidence of Colon Tumors

		WT		Min		
		Effective No. (male/female)	No. of mice with colon tumors (Incidence)	Effective No. (male/female)	No. of mice with colon tumors (Incidence)	WT vs. Min
Groups	A	12 (6/6)	0 (0%)	12 (10/2)	4 (33.3%)	p=0.09
	B	14 (7/7)	3 (21.4%)	9 (4/5)	9 (100%)	p<0.002
	C	17 (8/9)	0 (0%)	11 (4/7)	11 (100%)**	p<0.0001
	D	9 (3/6)	3 (33.3%)*	8 (3/5)	8 (100%)	p<0.001
	E	15 (9/6)	0 (0%)	7 (3/4)	7 (100%)	p<0.0001
	F	10 (5/5)	2 (20.0%)	6 (5/1)	6 (100%)	p<0.001

*p<0.05 vs. WT-C, **p<0.002 vs. Min-A

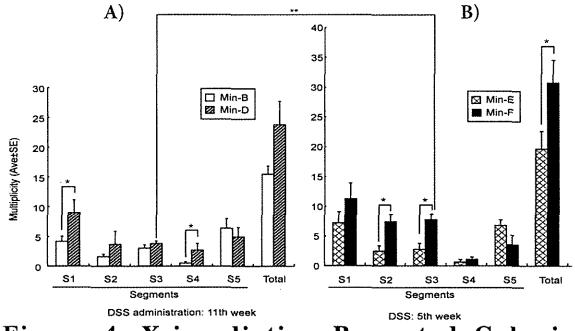

Figure 4. X-irradiation Promoted Colonic Tumorigenesis in DSS Treated Min mice. Group Min-B (Open bar), Min-D (Hatched bar), Min-E (Cross-hatched bar), and Min-F (Closed bar). *p<0.05 and **p<0.01

p<0.05) (Figure 3).

When 2% DSS was administered at 11 experimental week (Groups B and D), the number of colonic tumors were 8.88±2.20 (p<0.05) and 2.63±1.15 (p<0.05) in S1 and S4 in Group D, compared to 4.11±0.87 and 0.44±0.24, respectively, in Group B. It suggested enhancing effect of X-irradiation in Group D (Figure 4A).

If DSS was given at 5 week (Groups E and F), the numbers were 7.33±1.26 and 7.67±0.96 in S2 and S3, respectively, in Group F, compared with 2.43±0.87 and 2.71±1.04 in Group E, also indicating stimulating effect of X-irradiation in Group F (Figure 4B). Total numbers of colonic tumors was 30.67±3.83 and 19.57±2.9 in Groups F and E, respecively; the former was significantly higher than the latter (p<0.01).

When the two X-irradiation+DSS groups (Groups D and F in Figure 4 crossing left and right panels) were compared, earlier administration of DSS (7.67±0.96, Group F) was more effective in increment of colonic tumors in S3 compared to Group D (3.75±0.45) (p<0.05).

Multiplicity of colon tumors in WT mice

The number of total colonic tumors were 0.00±0.00, 0.50±0.27, 0.00±0.00, 0.78±0.46, 0.00±0.00, and 0.20±0.13/mouse in Groups A, B, C, D, E, and F, respecively, showing no significant differences among these groups.

Discussion

In the present study, we analyzed promoting effect of DSS-induced inflammation on X-irradiated colorectal carcinogenesis in WT and Min mice. Firstly, X-irradiation alone without DSS was assessed to confirm the effect of X-irradiation. In the Min mouse, incidence of colonic tumors was increased to 100% compared to non-irradiated group (33.3%). The number of colonic tumors in S2 was also increased with X-irradiation compared with non-irradiated Min mice. On the other hand, WT mice were not influenced with X-irradiation. It suggested that *Apc* locus might be more sensitive to loose normal APC function in Min mice although chromosome abberation might have occurred independent of their sequence (Rydberg, 1996). Okamoto and Yonekawa (Okamoto and Yonekawa, 2005) reported that 10 days old Min mice were more sensitive than other ages. In this study, since the mice were X-irradiated around 5 weeks old (35 days old), enhancing effect may have become unclear.

In the Min mice, DSS alone has known to enhance colonic tumorigenesis (Tanaka et al., 2006). X-irradiation was further added to assess if it may have enhanced colonic tumorigenesis. When Group F was compared with E, tumor multiplicity was increased in S2 and S3. Then, Group D vs. B, the number of tumors was increased upon X-irradiation in S1 and S4. Although localization of colonic tumors were different, X-irradiation was proved to exacerbate DSS-associated colonic tumorigenesis in Min mice. When the timing of DSS treatment was compared whether duration of inflammation could affect promoting effect, longer duration of inflammation had more enhancing effect (Group F) compared with shorter period (Group D). Similar phenomenon was observed in carcinogen induced murine colonic carcinogenesis model (Tanaka et al., 2003) and DSS alone induced model (Tanaka et al., 2006).

Considering WT mice, tumor incidence was increased in Groups D and F compared with non-treated or X-irradiation alone Groups, although enhancing effect was not as clear as that of Min mice. It was suggested that DSS treatment could bring latent genetic damage to apparent colonic tumors.

In the serial research in Life Span Study cohort of atomic bomb surviviors (Ozasa et al., 2012), the additive radiation risk of solid cancers continues to increase throughout life with a linear dose-response relationship. The estimated lowest dose range with a significant excessive relative risk (ERR) for all solid cancer was 0 to 0.20 Gy indicating no threshold. The risk of cancer mortality increased significantly for most major sites, including colon, whereas rectum did not. In the current study, multiplicities of colonic tumors (S2-S4 regions) were significantly increased with X-irradiation in Min-C (S2), Min-D (S4), and Min-F (S2 and S3) groups. In the

rectum (S1 region), although tumor multiplicity was not significantly different in DSS non-treated groups between Min-C and Min-A regardless of X-irradiation, Min-D receiving X-irradiation showed higher tumor multiplicity in the rectum compared with Min-B group. It suggested DSS-induced inflammation might have influenced rectal tumorigenesis as well as in colon.

Exposure to ionizing radiation is associated with an increased risk of cancer. The majority of radiation exposure and risk associated with gastrointestinal malignancy comes from CT scans, especially of the abdomen and pelvis; the colon carries the highest lifetime attributable risk of radiation associated malignancy (Chang and Hou, 2011). Besides patients, cancer risk of colon and rectum cancers in male diagnostic radiation workers in Korea also showed a significantly increasing trend according to the increase of the average annual radiation dose (HR: 2.37) (Choi et al., 2013).

Oncology patients treated for childhood cancer tended to develop secondary colorectal carcinomas. This risk was reported to be proportional to dose and volume of radiation; tumors were more likely localized in an irradiated segment of the colon (Nottage et al., 2012). Radiotherapy is a powerful tool for the treatment of gynecological malignancies including cervical (Tamai et al., 1999) and endemetrial cancers (Brown et al., 2010) and prostate cancer (Bolla et al., 2013). Patients treated with radiotherapy likely have significantly increased risk of subsequent primary malignancies including bladder, vagina, colon, and soft-tissue (Brown et al., 2010).

Low-level ionizing radiation (mean colon dose=0.18 Gy) has been revealed to influence the development of soft tissue sarcomas in atomic bomb survivors (Samartzis et al., 2013). However, no sarcomas were found in the current study, suggesting the DSS-induced inflammation has rarely affect stromal cells at least in this experimental condition.

In summary, our results suggest that colonic inflammation enhanced occult X-irradiated tumorigenesis not only in Min mice but also WT animals. It should be noted that those with colorectal inflammation including inflammatory bowel disease might exacerbate risk of colorectal cancer development in people with previous X-ray exposure. Patients should be carefully followed up especially with bowel inflammation.

Acknowledgements

This work was supported in part by a Grant-in-Aid for the Third-term Comprehensive 10-year Strategy for Cancer Control, a Grant-in-Aid for Cancer Research from the Ministry of Health, Labour and Welfare, Japan, and a Grant-in-Aid from Central Research Institute of Electric Power Industry (CRIEPI), Japan.

References

Balkwill F, Mantovani A (2001). Inflammation and cancer: back to Virchow? *Lancet*, **357**, 539-45.

Bolla M, Verry C, Long JA (2013). High-risk prostate cancer: combination of high-dose, high-precision radiotherapy and androgen deprivation therapy. *Curr Opin Urol*, **23**, 349-54.

Brown AP, Neeley ES, Werner T, et al (2010). A population-based study of subsequent primary malignancies after endometrial cancer: genetic, environmental, and treatment-related associations. *Int J Radiat Oncol Biol Phys*, **78**, 127-35.

Chang ML, Hou JK (2011). Cancer risk related to gastrointestinal diagnostic radiation exposure. *Curr Gastroenterol Rep*, **13**, 449-57.

Choi KH, Ha M, Lee WJ, et al (2013). Cancer risk in diagnostic radiation workers in Korea from 1996-2002. *Int J Environ Res Public Health*, **10**, 314-27.

Kinzler KW, Vogelstein B (1996). Lessons from hereditary colorectal cancer. *Cell*, **87**, 159-70.

Kohno H, Suzuki R, Sugie S, et al (2005). Beta-Catenin mutations in a mouse model of inflammation-related colon carcinogenesis induced by 1,2-dimethylhydrazine and dextran sodium sulfate. *Cancer Sci*, **96**, 69-76.

Luongo C, Dove WF (1996). Somatic genetic events linked to the Apc locus in intestinal adenomas of the Min mouse. *Genes Chromosomes Cancer*, **17**, 194-8.

Moser AR, Pitot HC, Dove WF (1990). A dominant mutation that predisposes to multiple intestinal neoplasia in the mouse. *Science*, **247**, 322-4.

Munkholm P (2003). Review article: the incidence and prevalence of colorectal cancer in inflammatory bowel disease. *Aliment Pharmacol Ther*, **18**, 1-5.

Nottage K, McFarlane J, Krasin MJ, et al (2012). Secondary colorectal carcinoma after childhood cancer. *J Clin Oncol*, **30**, 2552-8.

Ohshima H, Tatemichi M, Sawa T (2003). Chemical basis of inflammation-induced carcinogenesis. *Arch Biochem Biophys*, **417**, 3-11.

Okamoto M, Yonekawa H (2005). Intestinal tumorigenesis in Min mice is enhanced by X-irradiation in an age-dependent manner. *J Radiat Res*, **46**, 83-91.

Okayasu I, Hatakeyama S, Yamada M, et al (1990). A novel method in the induction of reliable experimental acute and chronic ulcerative colitis in mice. *Gastroenterology*, **98**, 694-702.

Ozasa K, Shimizu Y, Suyama A, et al (2012). Studies of the mortality of atomic bomb survivors, Report 14, 1950-2003: an overview of cancer and noncancer diseases. *Radiat Res*, **177**, 229-43.

Paulsen JE, Steffensen IL, Namork E, et al (2003). Age-dependent susceptibility to azoxymethane-induced and spontaneous tumorigenesis in the Min/+ mouse. *Anticancer Res*, **23**, 259-65.

Powell SM, Petersen GM, Krush AJ, et al (1993). Molecular diagnosis of familial adenomatous polyposis. *N Engl J Med*, **329**, 1982-7.

Rydberg B (1996) Clusters of DNA damage induced by ionizing radiation: formation of short DNA fragments. II. Experimental detection. *Radiat Res*, **145**, 200-9.

Samartzis D, Nishi N, Cologne J, et al (2013). Ionizing radiation exposure and the development of soft-tissue sarcomas in atomic-bomb survivors. *J Bone Joint Surg Am*, **95**, 222-9.

Shoemaker AR, Moser AR, Dove WF (1995) *N*-ethyl-*N*-nitrosourea treatment of multiple intestinal neoplasia (Min) mice: age-related effects on the formation of intestinal adenomas, cystic crypts, and epidermoid cysts. *Cancer Res*, **55**, 4479-85.

Steffensen IL, Paulsen JE, Eide TJ, et al (1997). 2-Amino-1-methyl-6-phenylimidazo[4,5-b]pyridine increases the numbers of tumors, cystic crypts and aberrant crypt foci in multiple intestinal neoplasia mice. *Carcinogenesis*, **18**, 1049-54.

Su LK, Kinzler KW, Vogelstein B, et al (1992). Multiple

intestinal neoplasia caused by a mutation in the murine homolog of the APC gene. *Science*, **256**, 668-70.

Tamai O, Nozato E, Miyazato H, et al (1999). Radiation-associated rectal cancer: report of four cases. *Dig Surg*, **16**, 238-43.

Tanaka T, Kohno H, Suzuki R, et al (2006). Dextran sodium sulfate strongly promotes colorectal carcinogenesis in Apc(Min/+) mice: inflammatory stimuli by dextran sodium sulfate results in development of multiple colonic neoplasms. *Int J Cancer*, **118**, 25-34.

Tanaka T, Kohno H, Suzuki R, et al (2003). A novel inflammation-related mouse colon carcinogenesis model induced by azoxymethane and dextran sodium sulfate. *Cancer Sci*, **94**, 965-73.

Tanaka T, Suzuki R, Kohno H, et al (2005). Colonic adenocarcinomas rapidly induced by the combined treatment with 2-amino-1-methyl-6-phenylimidazo[4,5-b]pyridine and dextran sodium sulfate in male ICR mice possess beta-catenin gene mutations and increases immunoreactivity for beta-catenin, cyclooxygenase-2 and inducible nitric oxide synthase. *Carcinogenesis*, **26**, 229-38.

Toyoda *et al. BMC Gastroenterology* 2013, **13**:122
http://www.biomedcentral.com/1471-230X/13/122

BMC Gastroenterology

RESEARCH ARTICLE Open Access

Gene expression analysis of a *Helicobacter pylori*-infected and high-salt diet-treated mouse gastric tumor model: identification of CD177 as a novel prognostic factor in patients with gastric cancer

Takeshi Toyoda[1,2†], Tetsuya Tsukamoto[3*†], Masami Yamamoto[4], Hisayo Ban[2], Noriko Saito[2], Shinji Takasu[1], Liang Shi[5], Ayumi Saito[6], Seiji Ito[7], Yoshitaka Yamamura[7], Akiyoshi Nishikawa[8], Kumiko Ogawa[1], Takuji Tanaka[9] and Masae Tatematsu[10]

Abstract

Background: *Helicobacter pylori* (*H. pylori*) infection and excessive salt intake are known as important risk factors for stomach cancer in humans. However, interactions of these two factors with gene expression profiles during gastric carcinogenesis remain unclear. In the present study, we investigated the global gene expression associated with stomach carcinogenesis and prognosis of human gastric cancer using a mouse model.

Methods: To find candidate genes involved in stomach carcinogenesis, we firstly constructed a carcinogen-induced mouse gastric tumor model combined with *H. pylori* infection and high-salt diet. C57BL/6J mice were given *N*-methyl-*N*-nitrosourea in their drinking water and sacrificed after 40 weeks. Animals of a combination group were inoculated with *H. pylori* and fed a high-salt diet. Gene expression profiles in glandular stomach of the mice were investigated by oligonucleotide microarray. Second, we examined an availability of the candidate gene as prognostic factor for human patients. Immunohistochemical analysis of CD177, one of the up-regulated genes, was performed in human advanced gastric cancer specimens to evaluate the association with prognosis.

Results: The multiplicity of gastric tumor in carcinogen-treated mice was significantly increased by combination of *H. pylori* infection and high-salt diet. In the microarray analysis, 35 and 31 more than two-fold up-regulated and down-regulated genes, respectively, were detected in the *H. pylori*-infection and high-salt diet combined group compared with the other groups. Quantitative RT-PCR confirmed significant over-expression of two candidate genes including *Cd177* and *Reg3g*. On immunohistochemical analysis of CD177 in human advanced gastric cancer specimens, over-expression was evident in 33 (60.0%) of 55 cases, significantly correlating with a favorable prognosis ($P = 0.0294$). Multivariate analysis including clinicopathological factors as covariates revealed high expression of CD177 to be an independent prognostic factor for overall survival.

(Continued on next page)

* Correspondence: ttsukamt@fujita-hu.ac.jp
†Equal contributors
[3]Department of Pathology, Fujita Health University School of Medicine, Toyoake, Japan
Full list of author information is available at the end of the article

(Continued from previous page)

Conclusions: These results suggest that our mouse model combined with *H. pylori* infection and high-salt diet is useful for gene expression profiling in gastric carcinogenesis, providing evidence that CD177 is a novel prognostic factor for stomach cancer. This is the first report showing a prognostic correlation between CD177 expression and solid tumor behavior.

Keywords: Cd177, Gastric cancer, *Helicobacter pylori*, Microarray, Salt

Background

Stomach cancer is the fourth most common cancer and second leading cause of cancer-related death worldwide [1]. *Helicobacter pylori* (*H. pylori*) is now recognized as a major risk factor for chronic gastritis and stomach cancer development [2]. In addition, environmental and host factors have also been shown to influence gastric carcinogenesis, and salt (sodium chloride, NaCl) and salty food are of particular importance, based on evidence from a number of epidemiological and experimental studies [3-6]. Thus, combined exposure to *H. pylori* infection and excessive salt intake appears to be very important for the development and progression of gastric tumors, although the detailed mechanisms, especially in terms of gene expression profiles, remain to be clarified.

High throughput microarray technology provides a powerful tool for comprehensive gene analysis, already applied to assess gene expression patterns in both human samples and animal models of gastric disorders [7-16]. Although many researchers have focused on gene expression in *H. pylori*-treated gastric cell lines [17-19], results in cell culture do not necessarily correlate with expression of specific genes in the *in vivo* microenvironment featuring host immune responses and stromal-epithelial interactions in cancers. Carcinogen-treated Mongolian gerbils have been used as a useful animal model of *H. pylori*-associated gastric carcinogenesis [20-24], and we previously reported that a synergistic interaction between *H. pylori* infection and high-salt intake accelerates chronic inflammation and tumor development in the stomachs of these animals [25,26]. Unfortunately, there is little information available for the gerbil genome, hampering genetic and molecular analysis. Therefore, attention has focused on mouse models [12,13], and establishment of a mouse model for stomach cancer featuring salt and *H. pylori* exposure is needed for investigations targeting genes involved in gastric carcinogenesis.

Previous microarray studies using rodent models did not distinguish and characterize expression profiles based on the interaction of *H. pylori* infection and salt intake. In the present study, we examined gene expression in the gastric mucosa in a *H. pylori*-infected and high-salt diet-treated mouse gastric tumor model by oligonucleotide microarray and found two candidate up-regulated genes including *Cd177* and *Reg3g*. We also investigated the expression of CD177 in human advanced gastric cancers by immunohistochemistry, and obtained evidence as a potential prognostic factor for stomach carcinogenesis.

Methods

Inoculation with *H. pylori*

H. pylori was prepared by the same method as described previously [27,28]. Briefly, *H. pylori* (Sydney strain 1) was inoculated on Brucella agar plates (Becton Dickinson, Cockeysville, MD, USA) containing 7% (v/v) heat-inactivated fetal bovine serum (FBS) and incubated at 37°C under microaerophilic conditions at high humidity for 2 days. Then, bacteria grown on the plates were introduced into Brucella broth (Becton Dickinson) supplemented with 7% (v/v) FBS and incubated under the same conditions for 24-h. After 24-h fasting, animals were intra-gastrically inoculated *H. pylori* (1.0×10^8 colony-forming units). Before inoculation, the broth cultures of *H. pylori* were checked under a phase-contrast microscope for bacterial shape and mobility.

Animals and experimental protocol

Fifty-six specific pathogen-free male, 5- or 6-week-old C57BL/6J mice (CLEA Japan, Tokyo, Japan) were used in this study. All animals were housed in plastic cages on hardwood-chip bedding in an air-conditioned biohazard room with a 12-h light/12-h dark cycle, and allowed free access to food and water throughout. The experimental design was approved by the Animal Care Committee of the Aichi Cancer Center Research Institute, and the animals were cared for in accordance with institutional guidelines as well as the Guidelines for Proper Conduct of Animal Experiments (Science Council of Japan, June 1st, 2006).

The experimental design is illustrated in Figure 1A. The mice were divided into 4 groups (Groups A-D); 21, 5, 15, and 15 mice were assigned to A, B, C, and D groups, respectively, at the commencement of the experiment. Animals of Groups B and D were inoculated with *H. pylori* intra-gastrically on alternate weeks (total 7 times), while mice of the other groups were inoculated with Brucella broth alone. All mice were given *N*-methyl-*N*-nitrosourea (MNU, Sigma Chemical, St Louis, MO, USA) in their drinking water at the concentration of 120 ppm on alternate weeks (total exposure was 5 weeks). For this purpose

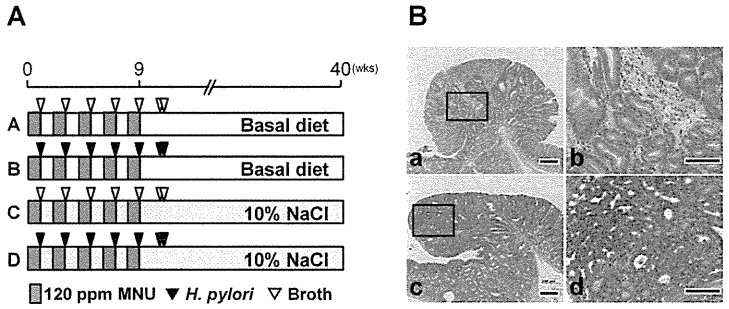

Figure 1 Experimental design and histopathological findings. A: Experimental design. Five- to six-week-old male C57BL/6J mice were inoculated with *H. pylori* SS1 strain (Groups B and D) or Brucella broth (Groups A and C). All animals were administered 120 ppm MNU in their drinking water on alternate weeks (total exposure, 5 weeks). Mice of Groups C and D were given basal diet (CE-2) containing 10% NaCl. **B**: Histopathological findings for MNU-induced mice gastric tumors. (a and b) Gastric adenoma in the pyloric region of an MNU-treated and *H. pylori*-infected mouse (Group B). (c and d) Gastric adenocarcinoma observed in Group B. Note the high cell density and cellular and structural atypia. Bar = 200 (a and c) or 100 μm (b and d).

MNU was freshly dissolved in distilled water three times per week. Mice of Groups C and D received CE-2 diets (basal sodium content of 0.36%; CLEA Japan) containing 10% NaCl. During the exposure period, one animal of Group B, one of Group C and six of Group D died or became moribund and they were excluded from the experiment. At 40 weeks, the remained animals were subjected to deep anesthesia and laparotomy with excision of the stomach.

Histological evaluation

For histological examination, the stomachs were fixed in 10% neutral-buffered formalin for 24-h, sliced along the longitudinal axis into strips of equal width, and embedded in paraffin. Four-μm thick sections were prepared and stained with hematoxylin and eosin (H&E) for histological observation. Tumors were classified into adenoma and adenocarcinoma based on cellular and morphological atypia and invasive growth to submucosa as we reported previously [21].

RNA preparation and oligonucleotide microarray analysis

Total RNA was extracted from the whole gastric mucosa including both tumor and peripheral tissue using an RNeasy Plus Mini Kit (Qiagen, Hilden, Germany) and its quality checked with a microchip electrophoresis system (i-chip SV1210; Hitachi Chemical, Tokyo, Japan). High-quality samples were selected, and pooled for each group to avoid individual difference for oligonucleotide microarray assessment (Group A, n = 3; B, n = 4; C, n = 6; D, n = 7). The CodeLink Mouse Whole Genome Bioarray (Applied Microarrays, Tempe, AZ, USA) containing 35,587 probe sets per chip was used to analyze gene expression profiles. Hybridization, processing, and scanning were performed by Filgen, Inc. (Nagoya, Japan), scan data images being analyzed using a software package (Microarray Data Analysis Tool, Filgen). Complete-linkage hierarchical clustering was also examined on the four groups using a qualified probe subset (Filgen).

Quantitative real-time RT-PCR of expression profiles in mice stomach

Relative quantitative real-time RT-PCR was performed using a StepOne Real-Time PCR System (Applied Biosystems, Foster City, CA, USA) with the mouse-specific glyceraldehyde-3-phosphate dehydrogenase (*Gapdh*) gene as an internal control. After DNase treatment, first strand cDNAs were synthesized from total RNA using a SuperScript VILO cDNA Synthesis Kit (Invitrogen, Carlsbad, CA, USA). The PCR was accomplished basically following the manufacturer's instructions using a QuantiTect SYBR Green PCR Kit (Qiagen). The primer sequences for each gene are listed in Table 1. Specificity of the PCR reactions was confirmed using a melt curve program provided with the StepOne software and electrophoresis of the PCR samples in 3% agarose gels. The expression levels of mRNAs were normalized to the mRNA level of *Gapdh* and compared with the control mice (Group A) by the ΔΔCT method.

Patients and tumor specimens

A total of 55 cases of primary advanced gastric cancer, surgically resected at Aichi Cancer Center Hospital (Nagoya, Japan) between 1995 and 2002, were investigated after obtaining informed consent. The study was approved by the ethics committee of Aichi Cancer Center. The patients were all male and the mean age and median follow-up period were 58.6 ± 10.2 years and 83 weeks, respectively. None had received preoperative chemotherapy or radiotherapy. Carcinomas with adjacent mucosa tissue were fixed and embedded in paraffin, and sectioned for staining

Table 1 Primer sequences for relative quantitative real-time RT-PCR

Gene	Sequences	Product length	Accession no.
Gapdh	5′-AACGGATTTGGCCGTATTG-3′	140	NM_008084
	5′-TTGCCGTGAGTGGAGTCATA-3′		
Cd177	5′-AGGGGTGCCACTCACTGTTA-3′	128	NM_026862
	5′-CCGATTGTTTTGGAGTCACC-3		
Reg3g	5′-GTATGGATTGGGCTCCATGA-3′	106	NM_011260
	5′-GATTCGTCTCCCAGTTGATG-3′		
Muc13	5′-CCTAATCCCTACGCAAACCA-3′	124	NM_010739
	5′-TCTGCCCATTTCTCCTTGTC-3′		

Gapdh glyceraldehyde-3-phosphate dehydrogenase, *Reg3g* regenerating islet-derived protein 3 gamma, *Muc13* mucin 13.

with H&E. Classification of tumor staging and diagnosis of advanced cases were made according to the Japanese Classification of Gastric Carcinomas [29]. The cancers had invaded the muscularis propria (T2 for TNM classification), the subserosa (T3), or the serosa and the peritoneal cavity (T4a), sometimes involving adjacent organs (T4b).

Immunohistochemistry using human gastric cancer tissue

We examined expression of CD177, for which a commercial primary antibody was available, in human gastric cancer tissues by immunohistochemistry. After inhibition of endogenous peroxidase activity by immersion in 3% hydrogen peroxide/methanol solution, antigen retrieval was carried out with 10 mM citrate buffer (pH 6.0) in a microwave oven for 10 min at 98°C. Then, sections were incubated with a mouse monoclonal anti-CD177 antibody (clone 4C4, diluted 1:100, Abnova, Taipei, Taiwan). Staining for CD177 was performed using a Vectastain Elite ABC Kit (Vector Laboratories, Burlingame, CA, USA) and binding visualized with 0.05% 3,3′-diaminobenzidine. The results of CD177 immunostaining in neoplastic cells were classified into four degrees; grade 0 (none, 0-10% of positive cells), grade 1 (weak, 10-30%), grade 2 (moderate, 30-60%), and grade 3 (strong, over 60%) based on proportion of stained cells, and cases showing moderate to strong staining were considered as positive.

Statistical analysis

The Chi-square test with Bonferroni correction was used to assess incidences of gastric tumor. Quantitative values including multiplicity of tumor and relative expression of mRNA were represented as means ± SD or SE, and differences between means were statistically analyzed by ANOVA or the Kruskal-Wallis test followed by the Tukey test for multiple comparisons. Overall survival was estimated using the Kaplan-Meier method and the log-rank test for comparisons. Correlations between CD177 expression and clinicopathological factors were analyzed by ANOVA or Chi-square test. Multivariate analysis was performed to examine whether CD177 over-expression was an independent prognostic factor using the Cox proportional-hazards regression model. P values of < 0.05 were considered to be statistically significant.

Results

Incidences and multiplicities of gastric tumors

The effective number of mice and the observed incidences and multiplicities of gastric tumors are summarized in Table 2. Tumors developed in the gastric mucosa of all MNU-treated groups (Groups A-D) (Figure 1B). In high-salt diet-treated groups (Groups C and D), the incidence of gastric tumor in Group D (*H. pylori*-infected; 100%) was significantly higher than that in Group C (non-infected; 50.0%) ($P < 0.05$). In basal diet groups (Groups A

Table 2 Incidence and multiplicity of gastric tumors in MNU-treated mice

Group	Effective number	Treatment	Incidence (%)			Multiplicity (no. of tumor/mouse)		
			Adenoma	Carcinoma	Total tumor	Adenoma	Carcinoma	Total tumor
A	21	MNU	3(14.3)	13(61.9)	13(61.9)	0.1 ± 0.4[a]	0.8 ± 0.7	0.9 ± 0.8
B	4	MNU + *H. pylori*	4(100)[b]	4(100)	4(100)	1.5 ± 0.6	1.8 ± 1.0	3.3 ± 1.0[c]
C	14	MNU + 10% NaCl	2(14.3)	6(42.9)	7(50.0)	0.2 ± 0.6	0.8 ± 1.0	1.0 ± 1.2
D	9	MNU + *H. pylori* + 10% NaCl	4(44.4)	8(88.8)	9(100)[d]	0.4 ± 0.5[e]	2.1 ±1.4[d]	2.6 ± 1.1[d]

Values for multiplicity are expressed as means ± SD. Incidences were generally assessed by Chi-square test, followed by pairwise analysis with Bonferroni correction. Multiplicities were generally analyzed by ANOVA, followed by the Tukey test for multiple comparison. [a]$P < 0.01$ *vs.* Group B, [b]$P < 0.01$ *vs.* Group A, [c]$P < 0.05$ *vs.* Group A, [d]$P < 0.05$ *vs.* Group C, [e]$P < 0.05$ *vs.* Group B.

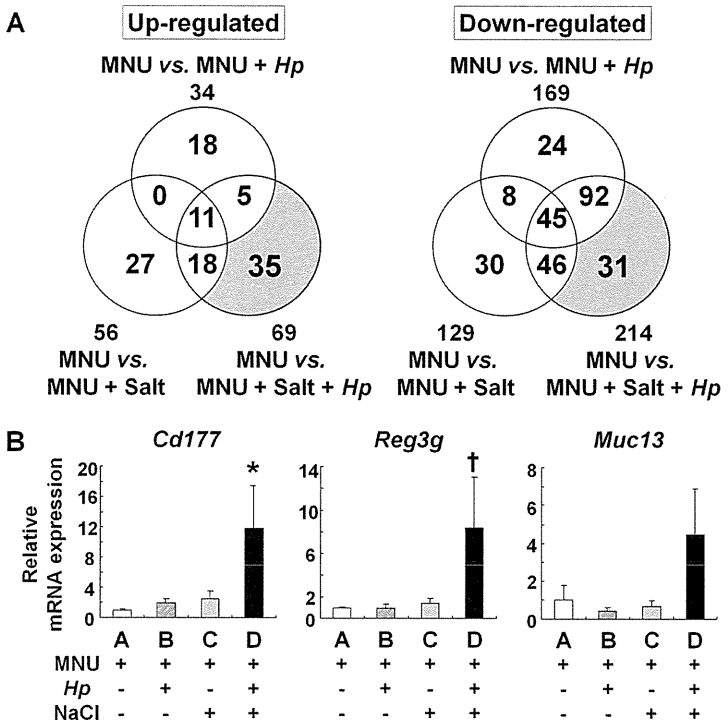

Figure 2 Global gene analysis in the glandular stomach of MNU-treated mice using oligonucleotide microarray. A: Number of genes up- or down-regulated more than two-fold in the stomach of MNU-treated mice. In Venn's diagram, the circles indicate up- (left) or down-regulated (right) genes in the stomach of MNU-treated mice with *H. pylori* infection, high-salt diet or their combination. The shaded area represents the up- or down-regulated genes more than two-fold only by the combination. **B**: Quantitative real-time RT-PCR analysis of three selected up-regulated genes (*Cd177*, *Reg3g*, and *Muc13*) in the stomachs of MNU-treated mice. Expression levels of the genes in each sample were normalized by *Gapdh* as internal control using ΔΔCT method. Relative expression levels were represented as the X-fold change relative to Group A (fixed as 1.0). Statistical analysis was performed by the Kruskal-Wallis test for general analysis and Tukey test for multiple comparison. Bars, SE; *, $P < 0.01$ *vs.* Group A and < 0.05 *vs.* Group C; †, $P < 0.01$ *vs.* Group C.

and B), the incidence was also increased by *H. pylori*-infection (Group A, 61.9% and Group B, 100%), albeit without statistical significance. The multiplicities of total tumors in both *H. pylori*-infected groups (Group B, 3.3 ± 1.0 tumors/mouse and Group D, 2.6 ± 1.1) were markedly higher than those in non-infected groups (Group A, 0.9 ± 0.8 and Group C, 1.0 ± 1.2) ($P < 0.05$). The multiplicity of gastric adenocarcinoma in Group D (2.1 ± 1.4) was slightly higher than that in Group B (1.8 ± 1.0) and significantly increased over the Group C value (0.8 ± 1.0) ($P < 0.05$). In contrast, the multiplicities of adenomas in Groups A and D (0.1 ± 0.4 and 0.4 ± 0.5, respectively) were significantly lower than in Group B (1.5 ± 0.6) ($P < 0.05$ and 0.01).

Gene expression profiling in the glandular stomachs by oligonucleotide microarray

With oligonucleotide microarrays, compared with the non-infected and basal diet-treated group (Group A), 34 genes were up-regulated and 169 were down-regulated more than two-fold in *H. pylori*-infected mice (Group B), 56 up-regulated and 129 down-regulated in high-salt diet-treated mice (Group C), and 69 up-regulated and 214 down-regulated in the combined group (Group D) (Figure 2A). Taken together, as shown in Table 3, we found that 35 genes were up-regulated and 31 genes were down-regulated more than two-fold only by the combination of *H. pylori* infection and high-salt diet. In addition, hierarchical clustering analysis was performed on the four groups with a total of 303 qualified probes using the complete-linkage clustering algorithm (Figure 3). Thirty-one probes including *Cd177*, *Reg3g* and *Muc13* were confirmed to be within a cluster of probes up-regulated only in Group D. Subsequent analysis in the present study was focused on these genes, because it was considered that the genes in which expression was altered only in the combined group might be associated with gastric carcinogenesis and progression in humans.

The entire results of this microarray analysis have been submitted and are readily retrievable from the

Table 3 Regulated genes by combination of *H. pylori* infection and high-salt diet in mouse gastric mucosa

Accession no.	Symbol	Genes/proteins	Fold changes
Up-regulated genes			
XM_357640	Igk-V8	Immunoglobulin kappa chain variable 8 (V8)	14.4
XM_001472541	Ighg	Immunoglobulin heavy chain (gamma polypeptide)	9.2
NM_026862	Cd177	CD177 antigen	7.3
NM_011260	Reg3g	Regenerating islet-derived 3 gamma	6.1
NM_023137	Ubd	Ubiquitin D	4.3
XM_144817	Igk-V34	Immunoglobulin kappa chain variable 34 (V34)	4.1
NM_007675	Ceacam10	Carcinoembryonic antigen-related cell adhesion molecule 10	3.7
NM_183322	Khdc1a	KH domain containing 1A	3.3
NM_011475	Sprr2i	Small proline-rich protein 2I	3.2
NM_175165	Tprg	Transformation related protein 63 regulated	3.2
NM_175406	Atp6v0d2	ATPase, H+ transporting, lysosomal V0 subunit D2	3.0
NM_009703	Araf	v-raf murine sarcoma 3611 viral oncogene homolog	2.6
NM_026822	Lce1b	Late cornified envelope 1B	2.5
NM_016958	Krt14	Keratin 14	2.5
NM_212487	Krt78	Keratin 78	2.4
NM_009807	Casp1	Caspase 1	2.4
NM_146037	Kcnk13	Potassium channel, subfamily K, member 13	2.4
NM_019450	Il1f6	Interleukin 1 family, member 6	2.3
NM_008827	Pgf	Placental growth factor	2.3
XM_893506	Klk12	Kallikrein related-peptidase 12	2.3
NM_016887	Cldn7	Claudin 7	2.3
NM_029360	Tm4sf5	Transmembrane 4 superfamily member 5	2.2
NM_172301	Ccnb1	Cyclin B1	2.2
NM_010739	Muc13	Mucin 13, epithelial transmembrane	2.2
NM_011165	Prl4a1	Prolactin family 4, subfamily a, member 1	2.2
NM_010162	Ext1	Exostoses (multiple) 1	2.2
NM_011704	Vnn1	Vanin 1	2.1
NM_011082	Pigr	Polymeric immunoglobulin receptor	2.1
NM_007769	Dmbt1	Deleted in malignant brain tumors 1	2.1
NM_022984	Retn	Resistin	2.1
NM_173037	Tmco 7	Transmembrane and coiled-coil domain 7	2.1
NM_009100	Rptn	Repetin	2.1
NM_007630	Ccnb2	Cyclin B2	2.1
NM_001081060	Slc9a3	Solute carrier family 9 (sodium/hydrogen exchanger), member 3	2.0
NM_146588	Olfr1030	Olfactory receptor 1030	2.0
Down-regulated genes			
NM_008753	Oaz1	Ornithine decarboxylase antizyme 1	0.31
NM_027126	Hfe2	Hemochromatosis type 2 (juvenile) (human homolog)	0.33
NM_053206	Magee2	Melanoma antigen, family E, 2	0.33
NM_010924	Nnmt	Nicotinamide N-methyltransferase	0.41
NM_026260	Tctn3	Tectonic family member 3	0.41
NM_181039	Lphn1	Latrophilin 1	0.43
NM_008312	Htr2c	5-hydroxytryptamine (serotonin) receptor 2C	0.43

Table 3 Regulated genes by combination of *H. pylori* infection and high-salt diet in mouse gastric mucosa *(Continued)*

NM_146667	Olfr740	Olfactory receptor 740	0.44
NM_007550	Blm	Bloom syndrome homolog (human)	0.44
NM_011243	Rarb	Retinoic acid receptor, beta	0.44
NM_184052	Igf1	Insulin-like growth factor 1	0.45
NM_013893	Reg3d	Regenerating islet-derived 3 delta	0.46
NM_008645	Mug1	Murinoglobulin 1	0.46
NM_029550	Keg1	Kidney expressed gene 1	0.46
NM_019388	Cd86	CD86 antigen	0.46
NM_011316	Saa4	Serum amyloid A 4	0.47
NM_007811	Cyp26a1	Cytochrome P450, family 26, subfamily a, polypeptide 1	0.47
NM_011538	Tbx6	T-box 6	0.48
NM_011086	Pip5k3	Phosphatidylinositol-3-phospate/phosphatidylinositol 5-kinase, type III	0.48
NM_133723	Asph	Aspartate-beta-hydroxylase	0.48
NM_001081390	Palld	Palladin, cytoskeletal associated protein	0.48
NM_007858	Diap1	Diaphanous homolog 1 (Drosophila)	0.48
NM_053271	Rims2	Regulating synaptic membrane exocytosis 2	0.48
NM_153163	Cadps2	Ca2+−dependent activator protein for secretion 2	0.49
NM_007541	Bglap1	Bone gamma carboxyglutamate protein 1	0.49
NM_031871	Ghdc	GH3 domain containing	0.49
NM_025545	Aptx	Aprataxin	0.49
NM_177322	Agtr1a	Angiotensin II receptor, type 1a	0.49
NM_026872	Ubap2	Ubiquitin-associated protein 2	0.49
NM_028045	Erv3	Endogenous retroviral sequence 3	0.49
NM_011641	Trp63	Transformation related protein 63	0.49

public database NCBI Gene Expression Omnibus (GEO) with the accession number GSE29444 (sample number: GSM728857-60).

Quantitative real-time RT-PCR analysis of gene expression profiles in MNU-treated mouse stomachs

Relative quantitative real-time RT-PCR analysis of three selected up-regulated genes (*Cd177*, *Reg3g*, and *Muc13*) in *H. pylori*-infected and high-salt diet-treated mice confirmed increased expression of *Cd177* and *Reg3g*, as shown in Figure 2B, with significant differences. Although expression level of *Muc13* in Group D was higher than all other groups, there was no statistical significance among them ($P = 0.0712$ *vs.* Group C).

Immunohistochemical expression of CD177 in human advanced gastric cancers and correlation with clinicopathological factors

On immunohistochemical analysis of human gastric cancer tissues, CD177 was observed not only in the membranes and cytoplasms of infiltrated neutrophils, but also in gastric cancer cells of both well- and poorly-differentiated adenocarcinomas (Figure 4A). Cancer cells of signet-ring cell type (2 cases) were negative for CD177. Among 55 gastric cancer cases, moderate to strong expression of CD177 was observed in 33 (60.0%) (Table 4).

The follow-up period of the patients ranged from 9 to 606 weeks (median = 83 weeks). Five-year survival rates for CD177-positive and negative were 39.4% and 18.2%, respectively. From the Kaplan-Meier survival curve analysis, CD177-positive expression was associated with better overall survival ($P = 0.0294$, log-rank test) (Figure 4B). There was no statistically significant correlation of CD177 expression with age, histological classification, depth of invasion, and lymph node metastasis (Table 4).

Multivariate analysis for overall survival of human gastric cancer cases

Using the Cox proportional hazards model, multivariate analysis of clinicopathological variables, including the patient age, tumor histological classification, invasion depth, lymph node metastasis, and CD177 expression (Table 5), revealed the last to be an independent factor for overall survival ($P = 0.0323$). Patient age and low

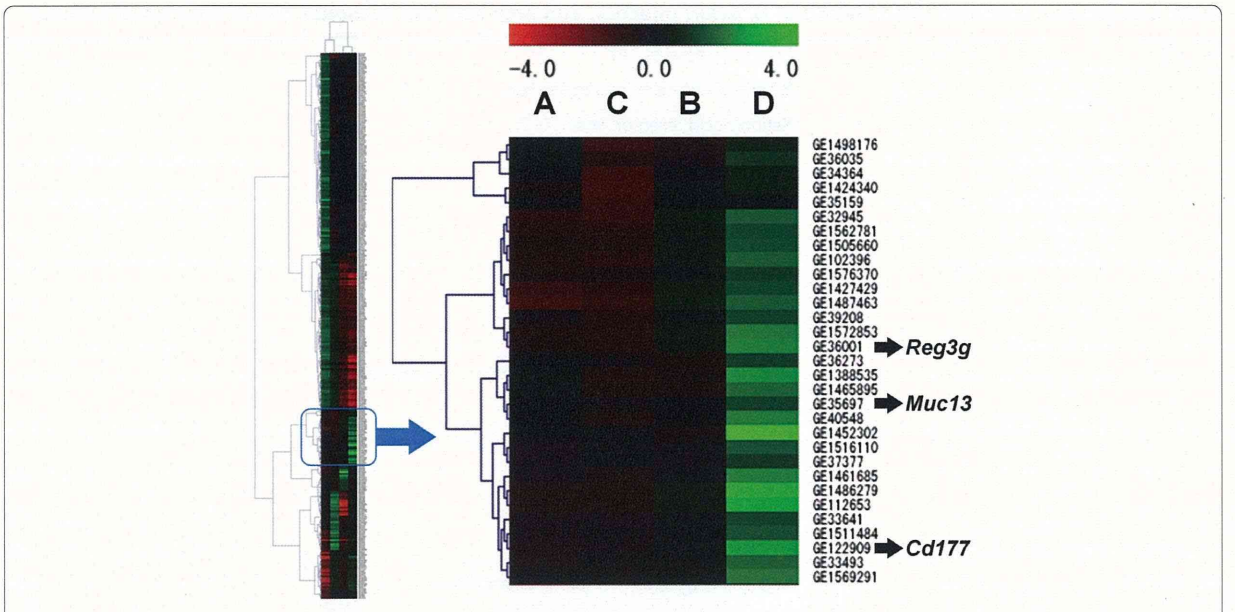

Figure 3 Hierarchical clustering analysis of four experimental groups of MNU-treated mice. Expression data from 303 qualified probes (left). The four experimental groups were classified into two clusters (Groups A/C) and (Groups B/D) based on similarities in expression patterns. Each row represents a probe and each column represents a experimental group (Groups A-D). As shown in the color bar, green indicates up-regulation; red indicates down-regulation; and black indicates no change. Thirty-one probes constituted a cluster of probes up-regulated only in Group D (right).

differentiation of adenocarcinoma were also associated with poor overall survival (P = 0.0439 and 0.0017, respectively). Tumor invasion depth and lymph node metastasis were not independent factors of gastric cancer cases in the present study ($P > 0.05$).

Discussion

In the present study, we demonstrated that the mouse model combined with *H. pylori* infection and high-salt diet is a useful tool to investigate the detailed mechanisms both of development and progression of gastric

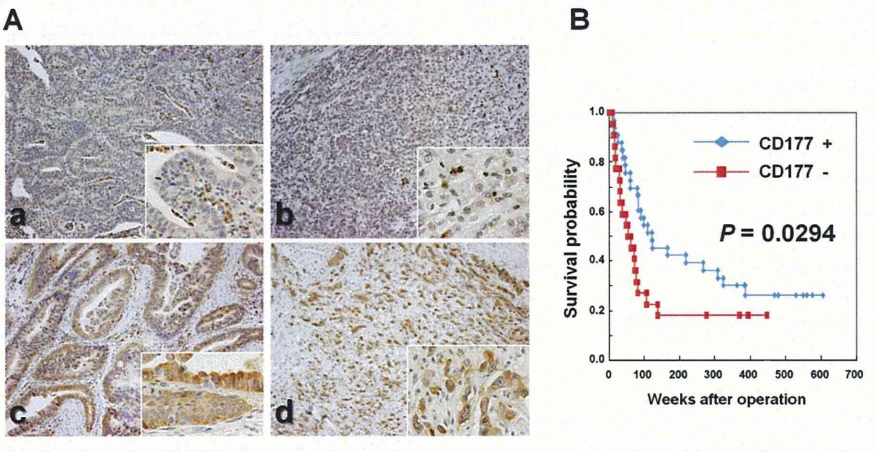

Figure 4 Immunohistochemistry for CD177 in human advanced gastric cancer and correlation with overall survival rate. A: Immunohistochemical analysis of CD177 expression in human gastric cancer tissue. (a and b) Negative staining (none to weak) for CD177 in a gastric adenocarcinoma. CD177 expression is present only in infiltrating neutrophils while neoplastic cells of well-differentiated (a) or poorly-differentiated (b) carcinoma are negative. Original magnification, ×100 (inset, ×400). (c and d) Note positive (moderate to strong) expression for CD177 in well-differentiated (c) or poorly-differentiated (d) gastric cancer cells. Original magnification, ×100 (inset, ×400). **B**: Comparison of Kaplan-Meier cumulative survival curves for CD177 negative and positive gastric cancer cases.

Table 4 CD177 expression in gastric carcinomas and its correlation with clinicopathological factors

	Case no.	CD177 Over-expression				*P* value‡
		Positive		Negative		
		Strong	Moderate	Weak	None	
Gastric adenocarcinomas	55	18	15	17	5	
Age						
Years (means ± SD)		55.3 ± 10.4	60.2 ± 8.13	59.8 ± 11.0	60.4 ± 13.0	0.5039
Histological classification						
Well/moderately-differentiated type*	21	6	9	4	2	0.1904
Poorly-differentiated/Signet-ring cell type**	34	12	6	13	3	
Depth of invasion†						
T1-3	27	5	10	10	2	0.2011
T4	26	11	5	7	3	
Lymph node metastasis						
N0	6	1	2	2	1	0.7869
N1-3	49	17	13	15	4	

* Lauren's intestinal type, ** Lauren's diffuse type, † Case number was reduced to fifty-three because the depth of invasion was not classified in two cases,
‡ ANOVA and Chi-square test were performed for age and other factors, respectively.

neoplasms. A number of rodent models of gastric cancer have been developed under various conditions, including *H. pylori* or *H. felis* infection, exposure to chemical carcinogens, and genetic modification [21,30]. Since *H. pylori* is known as a most closely-associated risk factor in man, animal models with infection of the bacterium, such as that utilizing Mongolian gerbils, are considered to be particularly important to mimic the background of human gastric carcinogenesis. On the other hand, there is a consensus that gastric cancer is a multifactorial disease [31]. Epidemiological studies and animal experiments have demonstrated that development of stomach cancer is also associated with many other factors including salt intake, alcohol drinking and cigarette, containing a wide variety of chemical carcinogen. In the present study, we attempted to mimic the gastric environment of human high-risk group exposed to combination of *H. pylori* infection, salt intake, and carcinogen.

As might be expected, there are both advantages and disadvantages of *Helicobacter*-infected mouse models. Instability of *cag* pathogenicity islands (PAI), a particularly important virulence factor of *H. pylori*, has been reported in the mouse model using SS1 strain [32]. Multiplicity of gastric tumors is difficult to examine in the gerbil model, because almost all of the stomach tumors in gerbils show invasive growth into the lamina propria or muscle layer. In the present study, our results demonstrated that *H. pylori* infection increased not only incidence but also multiplicity of gastric tumors in MNU-treated mice. Thus, the mouse model presented here has advantages in respect to investigate the multiplicity and tissue sampling for gene expression analysis.

In this study, we focused on the genes in which the expression was regulated only in *H. pylori*-infection and high-salt diet combined mice, which are expected to reflect the background of human high-risk group, to explore examples which might be associated with tumor progression. The two up-regulated genes selected, *Cd177* and *Reg3g* could be confirmed to exhibit significant over-expression by relative quantitative RT-PCR. Expression level of *Muc13* showed a tendency for increase with combination of *H. pylori* and salt, although this was not statistically significant. *Muc13* is a recently identified gene encoding transmembrane mucin that is expressed in the stomach to large intestine [33]. Shimamura et al. have reported that overexpression of *Muc13* is associated with differentiation towards the intestinal (differentiated) type of human gastric cancer [34]. In addition, the combined expression of

Table 5 Multivariate analysis of prognostic factos in patients with gastric cancer using Cox proportional hazard model

Factors	Hazard ratio	95% CI	*P* value
CD177 expression (negative)	2.07	1.063-4.021	0.0323
Age (year)	1.04	1.001-1.071	0.0439
Histological type (poorly-differentiated)	4.06	1.695-9.742	0.0017
Depth of invasion (high grade)	1.64	0.790-3.410	0.1838
Lymph node metastasis (positive)	3.40	0.773-14.92	0.1055

MUC13 with other metaplasia biomarkers is shown to be a prognostic indicator in several types of gastric cancer [35]. In the present study, all gastric tumors observed in MNU-treated mice were histologically of differentiated type. The REG protein family is also known to be associated with gastric cancer development and *Reg1α* and *Reg4* have been suggested as prognostic markers for advanced stomach cancers in man [36]. The present results indicate the possibility that *Reg3g* is also involved with progression of stomach tumor.

Immunohistochemical analysis of CD177 in advanced gastric cancer specimens showed expression to be significantly correlated with a good prognosis and survival rate after surgery. Importantly, multivariate analysis with clinicopathological factors as covariates further revealed high expression to be an independent prognostic factor for overall survival, as along with patient's age and histological classification. To our knowledge, the present study is the first to provide evidence that high expression of CD177 is associated with favorable prognosis in advanced gastric cancer.

CD177 is a member of the leukocyte antigen 6 (Ly-6) gene superfamily, encoding two neutrophil-associated proteins, NB1 and PRV-1 [37,38]. The NB1 glycoprotein is typically expressed on a subpopulation of neutrophils, located at plasma membranes and secondary granules. Recent studies have demonstrated that CD177 is overexpressed in neutrophils from 95% of patients with polycythemia vera and in half of patients with essential thrombocythemia [37]. Gonda et al. have reported a microarray analysis that *Cd177* expression in whole gastric tissue of *H. felis*-infected mice with mucosal dysplasia is reduced by folic acid supplementation [39]. Because they compared stage-matched groups to detect up- or down-regulated genes only by treatment of folic acid, it is unclear if *Cd177* expression is associated with gastritis or dysplasia. In our microarray results, there were no significant differences in expression of *Ela2*, which is a neutrophil-specific gene [40], and histological degrees of neutrophil infiltration were almost same among *H. pylori*-infected groups (data not shown). Therefore, the up-regulation of *Cd177* observed in this study was considered to be caused not by increased infiltration of neutrophils into the gastric mucosa but by a change of gene expression in tumor cells. NB1 is similar in structure to urokinase-type plasminogen activator receptor (uPAR), which is known to be associated with cell adhesion and migration [37]. Thus, there is a possibility that CD177 also acts as a regulator of adhesion and migration of neoplastic cells in gastric tumor. Further studies are needed to clarify the association between CD177 expression in gastric epithelial cells and tumor progression.

Conclusions

We demonstrated that the mouse model combined with *H. pylori* infection and high-salt diet is suitable for investigation of global gene expression associated with gastric tumor development and progression. Furthermore, our results suggest that CD177 expression might be associated with a favorable prognosis of gastric adenocarcinomas in man.

Abbreviations

FBS: Fetal bovine serum; *Gapdh*: Glyceraldehyde-3-phosphate dehydrogenase; H&E: Hematoxylin and eosin; *H. pylori*: *Helicobacter pylori*; Ly-6: Leukocyte antigen 6; MNU: *N*-methyl-*N*-nitrosourea; *Muc13*: Mucin 13; PAI: Pathogenicity islands; *Reg3g*: Regenerating islet-derived 3 gamma; RT-PCR: Reverse transcription-polymerase chain reaction; uPAR: Urokinase-type plasminogen activator receptor.

Competing interests

The authors declare that they have no competing interests.

Authors' contributions

TTo and TTs designed the study under the supervision of AN, KO, TTa and MT. MY, HB, NS, ST, LS and AS participated in the animal handling and procedures. Clinical sample collection and suggestions were provided by SI and YY. Sample analysis and evaluation were performed by TTo, TTs and MY. All authors read and approved the final manuscript.

Acknowledgements

This study was supported by Grant-in Aid for the Third-term Comprehensive 10-year Strategy for Cancer Control from the Ministry of Health, Labour and Welfare, Japan, Grant-in-Aid for the Cancer Research from the Ministry of Health, Labour and Welfare, Japan, and Grant-in-Aid for Young Scientists B (20790318 and 22700935) from the Ministry of Education, Culture, Sports, Science and Technology, Japan.

Author details

[1]Division of Pathology, National Institute of Health Sciences, Tokyo, Japan. [2]Division of Oncological Pathology, Aichi Cancer Center Research Institute, Nagoya, Japan. [3]Department of Pathology, Fujita Health University School of Medicine, Toyoake, Japan. [4]Faculty of Veterinary Medicine, Nippon Veterinary and Life Science University, Tokyo, Japan. [5]Chemicals Safety Department, Mitsui Chemicals Inc, Mobara, Japan. [6]Department of Pathology and Matrix Biology, Mie University Graduate School of Medicine, Tsu, Japan. [7]Department of Gastroenterological Surgery, Aichi Cancer Center Hospital, Nagoya, Japan. [8]Biological Safety Research Center, National Institute of Health Sciences, Tokyo, Japan. [9]The Tohkai Cytopathology Institute: Cancer Research and Prevention, Gifu, Japan. [10]Japan Bioassay Research Center, Hadano, Japan.

Received: 26 June 2012 Accepted: 22 July 2013
Published: 30 July 2013

References

1. Jemal A, Bray F, Center MM, Ferlay J, Ward E, Forman D: **Global cancer statistics.** *CA Cancer J Clin* 2011, **61**:69–90.
2. Uemura N, Okamoto S, Yamamoto S, Matsumura N, Yamaguchi S, Yamakido M, Taniyama K, Sasaki N, Schlemper RJ: ***Helicobacter pylori* infection and the development of gastric cancer.** *N Engl J Med* 2001, **345**:784–789.
3. Kono S, Hirohata T: **Nutrition and stomach cancer.** *Cancer Causes Control* 1996, **7**:41–55.
4. Tsugane S: **Salt, salted food intake, and risk of gastric cancer: epidemiologic evidence.** *Cancer Sci* 2005, **96**:1–6.
5. Joossens JV, Hill MJ, Elliott P, Stamler R, Lesaffre E, Dyer A, Nichols R, Kesteloot H: **Dietary salt, nitrate and stomach cancer mortality in 24 countries. European cancer prevention (ECP) and the INTERSALT cooperative research group.** *Int J Epidemiol* 1996, **25**:494–504.
6. Nozaki K, Shimizu N, Inada K, Tsukamoto T, Inoue M, Kumagai T, Sugiyama A, Mizoshita T, Kaminishi M, Tatematsu M: **Synergistic promoting effects of *Helicobacter pylori* infection and high-salt diet on gastric carcinogenesis in Mongolian gerbils.** *Jpn J Cancer Res* 2002, **93**:1083–1089.
7. Abe M, Yamashita S, Kuramoto T, Hirayama Y, Tsukamoto T, Ohta T, Tatematsu M, Ohki M, Takato T, Sugimura T, *et al*: **Global expression analysis of *N*-methyl-*N'*-nitro-*N*-nitrosoguanidine-induced rat stomach**

carcinomas using oligonucleotide microarrays. *Carcinogenesis* 2003, 24:861–867.
8. Hasegawa S, Furukawa Y, Li M, Satoh S, Kato T, Watanabe T, Katagiri T, Tsunoda T, Yamaoka Y, Nakamura Y: **Genome-wide analysis of gene expression in intestinal-type gastric cancers using a complementary DNA microarray representing 23,040 genes.** *Cancer Res* 2002, 62:7012–7017.
9. Boussioutas A, Li H, Liu J, Waring P, Lade S, Holloway AJ, Taupin D, Gorringe K, Haviv I, Desmond PV, *et al*: **Distinctive patterns of gene expression in premalignant gastric mucosa and gastric cancer.** *Cancer Res* 2003, 63:2569–2577.
10. El-Rifai W, Frierson HF Jr, Harper JC, Powell SM, Knuutila S: **Expression profiling of gastric adenocarcinoma using cDNA array.** *Int J Cancer* 2001, 92:832–838.
11. Hofman VJ, Moreilhon C, Brest PD, Lassalle S, Le Brigand K, Sicard D, Raymond J, Lamarque D, Hebuterne XA, Mari B, *et al*: **Gene expression profiling in human gastric mucosa infected with *Helicobacter pylori*.** *Mod Pathol* 2007, 20:974–989.
12. Kobayashi M, Lee H, Schaffer L, Gilmartin TJ, Head SR, Takaishi S, Wang TC, Nakayama J, Fukuda M: **A distinctive set of genes is upregulated during the inflammation-carcinoma sequence in mouse stomach infected by *Helicobacter felis*.** *J Histochem Cytochem* 2007, 55:263–274.
13. Takaishi S, Wang TC: **Gene expression profiling in a mouse model of *Helicobacter*-induced gastric cancer.** *Cancer Sci* 2007, 98:284–293.
14. Hippo Y, Taniguchi H, Tsutsumi S, Machida N, Chong JM, Fukayama M, Kodama T, Aburatani H: **Global gene expression analysis of gastric cancer by oligonucleotide microarrays.** *Cancer Res* 2002, 62:233–240.
15. Huff JL, Hansen LM, Solnick JV: **Gastric transcription profile of *Helicobacter pylori* infection in the rhesus macaque.** *Infect Immun* 2004, 72:5216–5226.
16. Vivas JR, Regnault B, Michel V, Bussiere FI, Ave P, Huerre M, Labigne A, DE MM, Touati E: **Interferon gamma-signature transcript profiling and IL-23 upregulation in response to *Helicobacter pylori* infection.** *Int J Immunopathol Pharmacol* 2008, 21:515–526.
17. Maeda S, Otsuka M, Hirata Y, Mitsuno Y, Yoshida H, Shiratori Y, Masuho Y, Muramatsu M, Seki N, Omata M: **cDNA microarray analysis of *Helicobacter pylori*-mediated alteration of gene expression in gastric cancer cells.** *Biochem Biophys Res Commun* 2001, 284:443–449.
18. Marcos NT, Magalhaes A, Ferreira B, Oliveira MJ, Carvalho AS, Mendes N, Gilmartin T, Head SR, Figueiredo C, David L, *et al*: ***Helicobacter pylori* induces beta3GnT5 in human gastric cell lines, modulating expression of the SabA ligand sialyl-Lewis x.** *J Clin Invest* 2008, 118:2325–2336.
19. Mills JC, Syder AJ, Hong CV, Guruge JL, Raaii F, Gordon JI: **A molecular profile of the mouse gastric parietal cell with and without exposure to *Helicobacter pylori*.** *Proc Natl Acad Sci USA* 2001, 98:13687–13692.
20. Tatematsu M, Nozaki K, Tsukamoto T: ***Helicobacter pylori* infection and gastric carcinogenesis in animal models.** *Gastric Cancer* 2003, 6:1–7.
21. Tsukamoto T, Mizoshita T, Tatematsu M: **Animal models of stomach carcinogenesis.** *Toxicol Pathol* 2007, 35:636–648.
22. Toyoda T, Tsukamoto T, Takasu S, Hirano N, Ban H, Shi L, Kumagai T, Tanaka T, Tatematsu M: **Pitavastatin fails to lower serum lipid levels or inhibit gastric carcinogenesis in *Helicobacter pylori*-infected rodent models.** *Cancer Prev Res* 2009, 2:751–758.
23. Toyoda T, Tsukamoto T, Takasu S, Shi L, Hirano N, Ban H, Kumagai T, Tatematsu M: **Anti-inflammatory effects of caffeic acid phenethyl ester (CAPE), a nuclear factor-kappaB inhibitor, on *Helicobacter pylori*-induced gastritis in Mongolian gerbils.** *Int J Cancer* 2009, 125:1786–1795.
24. Magari H, Shimizu Y, Inada K, Enomoto S, Tomeki T, Yanaoka K, Tamai H, Arii K, Nakata H, Oka M, *et al*: **Inhibitory effect of etodolac, a selective cyclooxygenase-2 inhibitor, on stomach carcinogenesis in *Helicobacter pylori*-infected Mongolian gerbils.** *Biochem Biophys Res Commun* 2005, 334:606–612.
25. Toyoda T, Tsukamoto T, Hirano N, Mizoshita T, Kato S, Takasu S, Ban H, Tatematsu M: **Synergistic upregulation of inducible nitric oxide synthase and cyclooxygenase-2 in gastric mucosa of Mongolian gerbils by a high-salt diet and *Helicobacter pylori* infection.** *Histol Histopathol* 2008, 23:593–599.
26. Kato S, Tsukamoto T, Mizoshita T, Tanaka H, Kumagai T, Ota H, Katsuyama T, Asaka M, Tatematsu M: **High salt diets dose-dependently promote gastric chemical carcinogenesis in *Helicobacter pylori*-infected Mongolian gerbils associated with a shift in mucin production from glandular to surface mucous cells.** *Int J Cancer* 2006, 119:1558–1566.
27. Shimizu N, Inada KI, Tsukamoto T, Nakanishi H, Ikehara Y, Yoshikawa A, Kaminishi M, Kuramoto S, Tatematsu M: **New animal model of glandular stomach carcinogenesis in Mongolian gerbils infected with *Helicobacter pylori* and treated with a chemical carcinogen.** *J Gastroenterol* 1999, 34(Suppl. 11):61–66.
28. Takasu S, Tsukamoto T, Cao XY, Toyoda T, Hirata A, Ban H, Yamamoto M, Sakai H, Yanai T, Masegi T, *et al*: **Roles of cyclooxygenase-2 and microsomal prostaglandin E synthase-1 expression and beta-catenin activation in gastric carcinogenesis in *N*-methyl-*N*-nitrosourea-treated K19-C2mE transgenic mice.** *Cancer Sci* 2008, 99:2356–2364.
29. Japanese Gastric Cancer Association: **Japanese Classification of Gastric Carcinoma - 2nd English Edition.** *Gastric Cancer* 1998, 1:10–24.
30. Oshima H, Oguma K, Du YC, Oshima M: **Prostaglandin E2, Wnt, and BMP in gastric tumor mouse models.** *Cancer Sci* 2009, 100:1779–1785.
31. Fock KM, Talley N, Moayyedi P, Hunt R, Azuma T, Sugano K, Xiao SD, Lam SK, Goh KL, Chiba T, *et al*: **Asia-Pacific consensus guidelines on gastric cancer prevention.** *J Gastroenterol Hepatol* 2008, 23:351–365.
32. Thompson LJ, Danon SJ, Wilson JE, O'Rourke JL, Salama NR, Falkow S, Mitchell H, Lee A: **Chronic *Helicobacter pylori* infection with Sydney strain 1 and a newly identified mouse-adapted strain (Sydney strain 2000) in C57BL/6 and BALB/c mice.** *Infect Immun* 2004, 72:4668–4679.
33. Williams SJ, Wreschner DH, Tran M, Eyre HJ, Sutherland GR, McGuckin MA: **Muc13, a novel human cell surface mucin expressed by epithelial and hemopoietic cells.** *J Biol Chem* 2001, 276:18327–18336.
34. Shimamura T, Ito H, Shibahara J, Watanabe A, Hippo Y, Taniguchi H, Chen Y, Kashima T, Ohtomo T, Tanioka F, *et al*: **Overexpression of MUC13 is associated with intestinal-type gastric cancer.** *Cancer Sci* 2005, 96:265–273.
35. Suh YS, Lee HJ, Jung EJ, Kim MA, Nam KT, Goldenring JR, Yang HK, Kim WH: **The combined expression of metaplasia biomarkers predicts the prognosis of gastric cancer.** *Ann Surg Oncol* 2012, 19:1240–1249.
36. Yamagishi H, Fukui H, Sekikawa A, Kono T, Fujii S, Ichikawa K, Tomita S, Imura J, Hiraishi H, Chiba T, *et al*: **Expression profile of REG family proteins REG Ialpha and REG IV in advanced gastric cancer: comparison with mucin phenotype and prognostic markers.** *Mod Pathol* 2009, 22:906–913.
37. Stroncek DF, Caruccio L, Bettinotti M: **CD177: A member of the Ly-6 gene superfamily involved with neutrophil proliferation and polycythemia vera.** *J Transl Med* 2004, 2:8.
38. Kissel K, Santoso S, Hofmann C, Stroncek D, Bux J: **Molecular basis of the neutrophil glycoprotein NB1 (CD177) involved in the pathogenesis of immune neutropenias and transfusion reactions.** *Eur J Immunol* 2001, 31:1301–1309.
39. Gonda TA, Kim YI, Salas MC, Gamble MV, Shibata W, Muthupalani S, Sohn KJ, Abrams JA, Fox JG, Wang TC, *et al*: **Folic acid increases global DNA methylation and reduces inflammation to prevent Helicobacter-associated gastric cancer in mice.** *Gastroenterology* 2012, 142:824–833.
40. Sturrock A, Franklin KF, Wu S, Hoidal JR: **Characterization and localization of the genes for mouse proteinase-3 (Prtn3) and neutrophil elastase (Ela2).** *Cytogenet Cell Genet* 1998, 83:104–108.

doi:10.1186/1471-230X-13-122
Cite this article as: Toyoda *et al.*: Gene expression analysis of a *Helicobacter pylori*-infected and high-salt diet-treated mouse gastric tumor model: identification of CD177 as a novel prognostic factor in patients with gastric cancer. *BMC Gastroenterology* 2013 13:122.

In Vivo Examination of the Genotoxicity of the Urban Air and Surface Soil Pollutant, 3,6-Dinitrobenzo[e]pyrene, with Intraperitoneal and Intratracheal Administration

Tatsuya Kato,[1,2] Yukari Totsuka,[2] Tomohiro Hasei,[3] Tetsushi Watanabe,[3] Keiji Wakabayashi,[1] Naohide Kinae,[1] Shuichi Masuda[1]

[1]Laboratory of Food Hygiene, Graduate School of Food and Nutritional Sciences, University of Shizuoka, 52-1 Yada, Suruga-ku, Shizuoka 422-8526, Japan

[2]Cancer Prevention Basic Research Project, National Cancer Center Research Institute, 1-1 Tsukiji 5-chome, Chuo-ku, Tokyo 104-0045, Japan

[3]Department of Public Health, Kyoto Pharmaceutical University, 5 Nakauchicho, Misasagi, Yamashina-ku, Kyoto 607-8414, Japan

Received 23 March 2011; revised 27 May 2011; accepted 4 June 2011

ABSTRACT: 3,6-Dinitrobenzo[*e*]pyrene (3,6-DNBeP) was identified as a new potent mutagen toward *Salmonella* strains in surface soil and airborne particles. Because data of *in vivo* examination of the genotoxicity of 3,6-DNBeP are limited, micronucleus test was performed in peripheral blood and bone marrow, and comet assay in the lungs of mice treated with 3,6-DNBeP. In male ICR mice intraperitoneally (i.p.) injected with 3,6-DNBeP, the frequency of micronuclated polychromatic erythrocytes (MNPCEs) was increased in the peripheral blood and bone marrow after 24 h in a dose-dependent manner. Compared to controls, the highest dose of 3,6-DNBeP (40 mg/kg B.W.) induced 7.3- and 8.7-fold increases of MNPCE frequency in the peripheral blood and bone marrow, respectively. Furthermore, when 3,6-DNBeP was intratracheally (i.t.) instilled to male ICR mice, 3,6-DNBeP at the highest dose of 0.1 mg/kg body exhibited 3.1-fold increase of DNA tail moment in the lungs at 3 h after the instillation compared to controls. The values of DNA tail moment at 9 and 24 h after the instillation were increased up to 3.5 and 4.2-fold, respectively. These data indicate that 3,6-DNBeP is genotoxic to mammalians in *in vivo* and suggest that 3,6-DNBeP may be a carcinogenic compound present in the human environment. Environ Toxicol 28: 588–594, 2013.

Keywords: 3,6-dinitrobenzo[*e*]pyrene; genotoxicity; surface soil; intratracheal instillation; nitro-PAHs

INTRODUCTION

Many kinds of chemicals are released into the atmospheric environment from diesel exhaust, waste incineration plants, and so on and are adsorbed to atmospheric particles (Leiter et al., 1942; Siak et al., 1985; Lewtas et al., 1990). Some of them including polycyclic aromatic hydrocarbons (PAHs) and nitrated PAHs (nitro-PAHs) show mutagenic and/or carcinogenic activities (Stenberg et al., 1983). Atmospheric

Correspondence to: S. Masuda; e-mail: masudas@u-shizuoka-ken.ac.jp

Contract grant sponsors: Ministry of Health, Labour and Welfare, Japan (the U.S. Japan Cooperative Medical Science Program, a Grant-in-Aid for Cancer Research) and The Sumitomo Foundation.

Published online 24 August 2011 in Wiley Online Library (wileyonlinelibrary.com). DOI 10.1002/tox.20754

particles precipitate into the ground surface to some extent, and the surface soil is contaminated with these genotoxic compounds (Hasei et al., 2006). In fact, surface soils from parks (Nishimura et al., 1984; Watanabe et al., 2005b), agricultural land (Brown et al., 1985), roadsides (Arashidani et al., 1992), and residential sites (Knize et al., 1987; Watanabe et al., 2003) are reported to exhibit genotoxic activity.

Nitro-PAHs are released during combustion processes by diesel engines, wood-burning, (Rosenkrantz et al., 1982; Gibson, 1983) and so forth and are formed secondarily by the reaction of PAHs with nitrogen oxide in the atmosphere (Tokiwa et al., 1981). Nitro-PAHs are of enormous concern because of their genotoxicity (Tokiwa and Ohnishi, 1986) and ubiquity in the atmospheric environment (Gibson, 1983). Especially, 1,3-, 1,6-, and 1,8-dinitropyrene (DNP) isomers have been examined with great attention, because these compounds show highly mutagenic activity in bacteria (Tokiwa and Ohnishi, 1986) and cultured mammalian cell lines (O'Donocan et al., 1990) and have exhibited carcinogenicity in experimental animals (Takayama et al., 1985).

Recently, we found a new nitro-PAH as a novel mutagen from surface soil collected at Takatsuki city in Osaka Prefecture and four other cities, and the compound was identified as 3,6-dinitrobenzo[*e*]pyrene (3,6-DNBeP) (Watanabe et al., 2005a). Extracts of these surface soils exhibited potent mutagenicity in the Ames/*Salmonella* assay, and 3,6-DNBeP also showed significant mutagenic activity in *Salmonella typhimurium* TA98 without the metabolic activation system (S9 mix), inducing 285,000 revertants/nmol. The potency is equivalent to those of DNP isomers that have been classified as possible human carcinogens (group 2B) by IARC (1989; 1996). In addition, using a sensitive method with a reducer column and a fluorescence detector for quantifying 3,6-DNBeP in surface soil and airborne particles (Hasei et al., 2006), 3,6-DNBeP was detected in surface soil and airborne particles with the range of 347-5007 pg/g for soil and 137-1238 fg/m^3 for airborne particles. The contribution ratios of 3,6-DNBeP toward total mutagenicity of soil extracts in *S. typimurium* TA98 without S9 mix were from 16.5 to 30.6%, and the amounts of 3,6-DNBeP in both surface soil and airborne particles were comparable to those of DNP isomers. Therefore, it is important to evaluate the genotoxicity of 3,6-DNBeP in assays other than Ames/*Salmonella* assay. Kawanishi et al. (2009) reported that treatment of HepG2 cells with 3,6-DNBeP indicated mutagenic and genotoxic activity in *hprt* mutation assay, sister chromatid exchange test, and micronucleus test. Moreover, the DNA damaging potency of 3,6-DNBeP was observed in ICR mice intraperitoneally (i.p.) injected with this compound, as shown by comet assay (Kawanishi et al., 2009).

In the present study, in order to further evaluate the *in vivo* genotoxicity of 3,6-DNBeP, micronucleus test was performed using peripheral blood and bone marrow derived from ICR mice i.p. injected with 3,6-DNBeP. Moreover, because 3,6-DNBeP is present in atmospheric environment, DNA damaging activity of 3,6-DNBeP was examined using the lungs of mice intratracheally (i.t.) instilled with this compound. Genotoxic activity of 3,6-DNBeP was detected in both assay systems, and its potency was comparable to those of other air pollutants, DNP isomers. Possible carcinogenic potency of 3,6-DNBeP is also discussed.

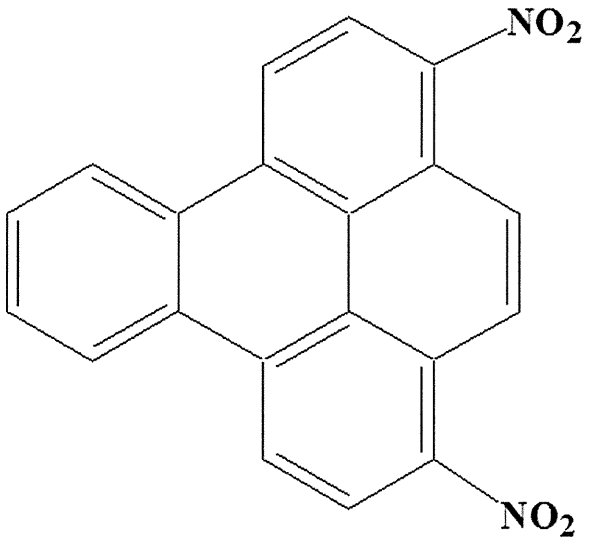

Fig. 1. Chemical structure of 3,6-DNBeP.

MATERIALS AND METHODS

Materials

3,6-DNBeP was synthesized as described previously (Watanabe et al., 2005a). Figure 1 shows the chemical structure of 3,6-DNBeP. Corn oil, glyceryltrioctanoate, low melting point (LMP) and normal melting point (NMP) agarose, dimethyl sulfoxide, and Triton X-100 were purchased from Sigma-Aldrich (St. Louis, MO). Halothane was from Takeda Pharmaceutical Company (Osaka, Japan). Fetal bovine serum (FBS) was taken from Gibco-BRL (Grand Island, NY). Ethidium bromide was obtained from Merck (Darmstadt, Germany), and all other chemicals were from Wako Pure Chemicals (Osaka, Japan).

Animals

Eight-week-old male ICR mice were obtained from Japan SLC (Shizuoka, Japan) and used for experiment when 9 weeks old. Food (CE-2 commercial diet: Japan Clea Co., Tokyo, Japan) and water were given freely. The room in which mice were placed was air conditioned at 23°C with a light/dark (12-h) cycle. The experiments were conducted

according to the Guidelines for Animal Experiments in the National Cancer Center and the Guidelines of the University of Shizuoka for the Care and Use of the Laboratory Animals.

Micronucleus Test Using Peripheral Blood and Bone Marrow

Two doses (20 and 40 mg/kg B.W.) of 3,6-DNBeP dissolved in corn oil were i.p. administrated to mice ($n = 5$). Only corn oil was also injected as vehicle control. The animals were sacrificed 24 and 48 h after administration, and peripheral blood and bone marrow were obtained. Peripheral blood and bone marrow were used for the micronucleus test.

The micronucleus test was performed according to the method of Hayashi et al. (Hayashi et al., 1994) with some modifications. Five microliters of peripheral blood were diluted with the same volume of FBS. Five microliters of diluted blood were spread on an acrydine orange-coated glass slide, covered with a coverslip, and supravitally stained. Within a few days of slide preparation, 1000 polychromatic erythrocytes (PCEs) were observed with a fluorescence microscope (Nikon ECLIPSE 80i fluorescence microscope: magnification, 1000×) and the numbers of micronuclated PCEs (MNPCEs) were recorded. Bone marrow samples were cleaned-out with 1 mL FBS, and cells were collected by centrifugation. The volumes of supernatants were adjusted to the same volume of deposition, and the supernatants were mixed with pipetting. Five microliters of cell suspension were smeared on a clean slide with a cover glass, and the slides were dehydrated with 70% ethanol to fixate. Then, the slides were stained with 40 μg/mL acridine orange just before microscopical observation, 1000 PCEs were observed with a fluorescence microscope (magnification, 400×), and the numbers of MNPCE were recorded. At the same time, the numbers of PCEs in 1000 normochromatic erythrocytes (NCEs) were counted.

Alkaline Comet Assay Using the Lungs Obtained from Mice After i.t. Instillation with 3,6-DNBeP

Two doses (0.05 and 0.1 mg) of 3,6-DNBeP dissolved in 50 μL glyceryltrioctanoate were i.t instilled to mice ($n = 5$) using a polyethylene tube under anesthesia with 4% halothane. Only glyceryltrioctanoate also was i.t. instilled as vehicle control ($n = 5$). Mice were sacrificed at 3, 9, and 24 h after 3,6-DNBeP injection, and the lungs were circulated with saline and subsequently taken for the comet assay.

The lungs were minced and suspended with chilled homogenizing buffer [30 mM EDTA-2Na and 0.9% KCl (v/v)] and homogenized gently using a Dunce-type homogenizer on ice to gain the single-cell suspensions.

The alkaline comet assay was carried out by the method described previously with some modifications (Singh et al., 1988; Toyoizumi et al., 2008). Briefly, to make slide coated with a first agarose layer, 75 μL of 0.7% NMP agarose in phosphate buffer saline (PBS) was spread on a clear frosted slide and allowed to dry overnight. Seventy-five microliters of cell suspension were mixed with the same volume of 1.4% LMP agarose in PBS. The mixture (75 μL) was layered on a first agarose layer and covered with 75 μL of 0.7% LMP agarose. After slide preparation, the slide was immersed in lysing solution (2.5 M NaCl, 0.1 M EDTA-2Na, 0.01 M Tris base, 1% salcosinate-NaOH buffer, 10% dimethyl sulfoxide and 1% Triton X-100, and pH 10) and refrigerated at 0°C for 1 h. Each slide was then placed in alkaline electrophoresis buffer (0.3 M NaOH and 1 mM EDTA-2Na) for 10 min to allow for DNA unwinding. Electrophoresis was performed at 25 V, 300 mA for 15 min at 4°C. The slides were neutralized with Tris buffer (0.4 M Tris base, pH 7.5) for 5 min twice and dehydrated with 70% ethanol to fixate. The cells were stained with 50 μL of ethidium bromide solution (20 μg/mL). Comet images were analyzed using a fluorescence microscope (magnification 200×) equipped with a CCD camera. Fifty cells were examined per one plate. The tail moment of DNA was measured using Comet Analyzer from Youworks Co. (Ibaraki, Japan).

Statistical Analysis

Dunnett's test after one-way ANOVA was used to evaluate the significance of differences of MN frequency in the micronucleus test and DNA tail moment in the comet assay between groups treated with 3,6-DNBeP and control groups; P values lower than 0.05 were considered to indicate statistical significance.

RESULTS

Clastogenic Activity in Peripheral Blood and Bone Marrow by i.p. Administration of 3,6-DNBeP

To evaluate the clastogenic activity, the micronuclei induction by i.p. administration of 3,6-DNBeP was measured. Peripheral blood and bone marrow taken at 24 and 48 h after administration were subjected to the micronucleus test. Figure 2 and Table I show the frequency of MNPCEs in peripheral blood. The dose-dependent increase of frequency was observed at 24 h after administration of 3,6-DNBeP. Compared to vehicle control, frequencies increased 5.0 ($P < 0.05$) and 7.3 ($P < 0.01$) fold with 20 and 40 mg/kg, respectively. In the case of 48 h, MNPCE frequency decreased by 64% with high dose compared to that observed at 24 h after the administration, whereas no

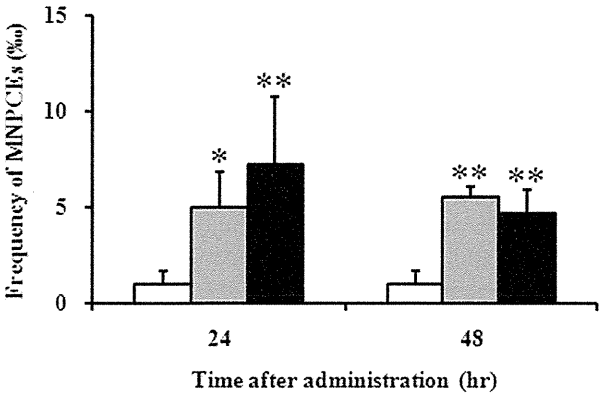

Fig. 2. Clastogenic activity of 3,6-DNBeP in peripheral blood. Mice were i.p. injected with 3,6-DNBeP at doses of 20 (gray bar) and 40 mg/kg B.W. (black bar). Control mice were injected with corn oil (open bar). One thousand PCEs were observed per mouse. The values represent the mean of five animals ± SD. *$P < 0.05$, ** $P < 0.01$ (vs. control).

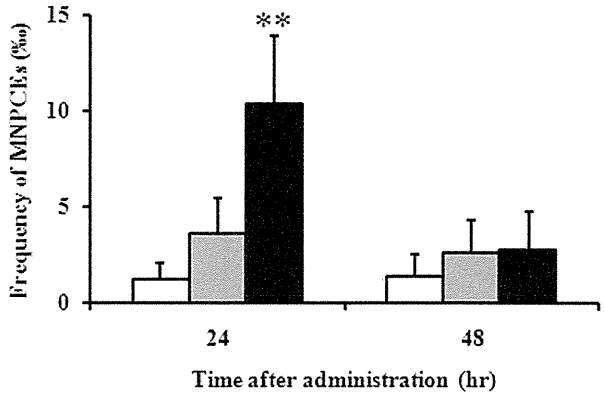

Fig. 3. Clastogenic activity of 3,6-DNBeP in bone marrow. Mice were i.p. injected with 3,6-DNBeP at doses of 20 (gray bar) and 40 mg/kg B.W (black bar). Control mice were injected with corn oil (open bar). One thousand PCEs were observed per mouse. The values represent the mean of five animals ± SD. *$P < 0.05$, ** $P < 0.01$ (vs. control).

notable changes of MNPCE frequencies were observed at low dose between two sampling times.

As shown in Figure 3, MNPCE frequency increased more markedly in bone marrow than in peripheral blood ($P < 0.01$) with high dose 24 h after the administration. No significant increase was detected with both doses after 48 h.

Cytotoxicity of 3,6-DNBeP Against Hematopoietic Tissues

Concomitantly with micronucleus test, the numbers of PCEs in 1000 NCEs, as a cytotoxicity against hematopoietic tissues induced by i.p. injection with 3,6-DNBeP, were counted. The number of PCEs in 1000 NCEs decreased in a dose- and time-dependent manner (Table I). The decrease of the number of PCEs was most prominent at 48 h after the administration with high dose of 3,6-DNBeP ($P < 0.01$).

TABLE I. The frequency of MNPCEs per 1000 PCEs and PCEs per 1000 NCEs in peripheral blood

	Frequency of MNPCEs (‰)		Frequency of PCEs (‰)	
	24 h	48 h	24 h	48 h
Control	1.0 ± 0.7	1.0 ± 0.7	58.6 ± 5.7	57.4 ± 4.7
3,6-DNBeP (20 mg/kg)	5.0 ± 1.9[a]	5.5 ± 0.6[b]	51.4 ± 4.9	46.8 ± 4.1[a]
3,6-DNBeP (40 mg/kg)	7.3 ± 3.5[b]	4.7 ± 1.2[b]	42.4 ± 8.1[b]	16.8 ± 3.7[b]

The PCEs/NCEs ratios were obtained concomitantly with the micronucleus test. The PCEs/NCEs ratios reflect the cytotoxicity of chemicals against hematopoietic systems. These values represent the mean of five animals ± SD.

[a] $P < 0.05$.

[b] $P < 0.01$ (vs. control).

DNA Damaging Potency in the Lungs by i.t. Instillation of 3,6-DNBeP

DNA damaging potency of 3,6-DNBeP in the lungs of mice was evaluated using the comet assay under alkaline conditions. Figure 4(a) shows the mean values of DNA tail moment in the lungs of mice treated with 3,6-DNBeP at 0.05 and 0.1 mg/mouse for 3 h. The DNA damages were dose-dependent, and the values of DNA tail moment were significantly increased as compared with that from control mice. DNA damage against vehicle control was increased 2.4 ($P < 0.01$) and 3.1 ($P < 0.01$) fold with the low and high doses of 3,6-DNBeP, respectively. Furthermore, we examined the DNA damage in the lungs at three time points after i.t. instillation, i.e., 3, 9, and 24 h at 0.1 mg of 3,6-DNBeP/mouse. As shown in Figure 4(b), the highest DNA tail moment was detected when the tissue was removed at 24 h after the instillation, whereas no time-dependent increase of the tail moment was shown in the control animals.

DISCUSSION

In the present study, we found that 3,6-DNBeP, which is isolated from surface soil and airborne particles as one of the major mutagens in *Salmonella*, showed *in vivo* genotoxic activity in micronucleus test and comet assay in mice.

The micronucleus test is widely used as a screening method for detecting the clastogenicity of chemicals. Hayashi et al. (1994) introduced a method for the observation of micronucleated young erythrocytes using supravital staining with acridine orange. This method can detect very young micronucleated erythrocytes in the peripheral blood

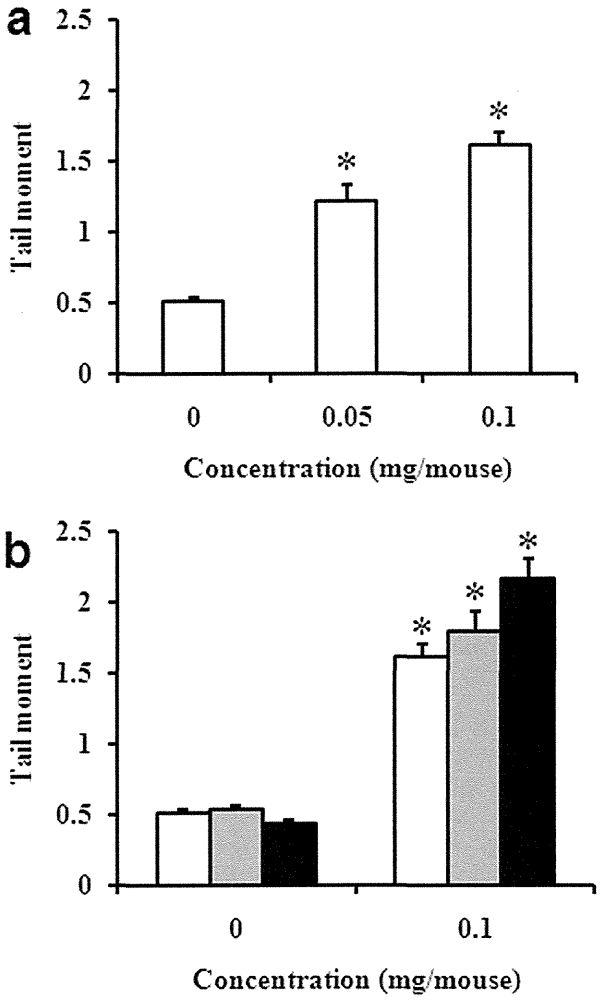

Fig. 4. DNA damaging potency of 3,6-DNBeP in the lungs by i.t. instillation. Mice were i.t. instilled with 3,6-DNBeP at doses of 0.05 and 0.1 mg/mouse. Control mice were treated with glyceryltrioctanoate. Mice were sacrificed at 3 (open bar), 9 (gray bar), and 24 h (black bar) after instillation. The tail moment is shown in a and b with doses and time course, respectively. The values represent the mean of five animals ± SEM. *$P < 0.01$ (vs. control).

stream before being trapped and destroyed by the spleen. Two doses (20 and 40 mg/kg B.W.) of 3,6-DNBeP were i.p. injected to ICR mice, and the mice were dissected at 24 and 48 h after injection. The dose-dependently increased MNPCEs were observed at 24 h after injection in both peripheral blood and bone marrow. In the peripheral blood, the MNPCEs at higher dose decreased at 48 h when compared with 24 h, whereas those at lower dose remained unchanged. According to the data of Vrzocand and Petras, when *N*-methyl-*N*-nitrosourea (MNU) was i.p. administrated at extremely high dose of 150 mg/kg B.W. in male BALB/cBtJ mice, MNPCEs were hardly observed in the peripheral blood of mice at 48 h after administration (Vrzoc et al., 1997). Because almost no observation of MNPCEs was thought to be due to the damages caused by MNU in hematopoietic systems, the decrease of MNPCEs with higher dose of 3,6-DNBeP may also be due to the same damages. In fact, our data showed that the number of PCEs in 1000 NCEs was decreased by i.p. injection at dose of 40 mg/kg B.W. at 48 h after the administration, suggesting that 3,6-DNBeP may show strong toxicity to hematopoietic tissues. Consistent with these observations, in bone marrow, the MNPCEs were dominantly increased in higher dose for 24 h and reduced until spontaneous level at 48 h after instillation. Previous studies showed that treatment of CHL cells with 0.25 μg/mL of 1,8-DNP and 0.2μg/mL of 3,6-DNBeP increased the frequencies of micronucleated cells about 11.5 and 2.5 times higher than the background level, respectively (Watanabe et al., 1994; Kawanishi et al., 2009). Moreover, 1,8-DNP exhibited carcinogenicity in BALB/c mice (Otohuji et al., 1987).

Because 3,6-DNBeP is thought to be mainly present in ambient air, we injected by i.t. instillation to investigate the genotoxicity of 3,6-DNBeP in the lungs by using the comet assay. The comet assay was developed by Singh et al. (1988), and this method has a high sensitivity for detecting low levels of DNA damage in individual cells (Speit et al., 2004). Moreover, it requires small numbers of cells per sample and short time to complete a study. Inhalation experiments are the best way to estimate the effects of inhaled gas, dust, and chemicals, but require not only considerable amounts of materials, but also a safe and well-controlled system for exposure and maintenance of animals (Nagy et al., 2005). Thus, i.t. instillation is a useful method as a model for inhalation. The increased tail moment values were observed by i.t. instillation of 3,6-DNBeP, and the highest genotoxic activity was found at 24 h after instillation. It has been reported that DNA damage in the liver, kidneys, lungs, and bone marrow of ICR mice was induced by i.p. injection of 3,6-DNBeP (20, 40, and 80 mg/kg B.W.), and the values of Tail moment in lungs were about 1.5 (Kawanishi et al., 2009). In the present study, almost the same DNA damaging potency was observed in the lungs even though the dose of 3,6-DNBeP was quite low (about 2.5 mg/kg B.W.). It is thought that the administration route could influence the distribution (concentration) of 3,6-DNBeP in the lungs. Because 3,6-DNBeP could be spread into several tissues by i.p. injection, the amount of 3,6-DNBeP reaching the lungs might be only a part, whereas almost the whole amount of 3,6-DNBeP could be retained in the lungs by i.t. instillation. Thus, the DNA damaging potency in the present study may be the same as that of the previous report. Moreover, we determined the DNA damaging potency induced by i.p. injection of 3,6-DNBeP at the doses of 20 and 40 mg/kg B.W. in the same manner of Kawanishi et al. (2009) and observed similar data (data not shown). Another previous study showed that

the increased levels of DNA adducts derived from 1,6-DNP were observed at 24 h after direct administration to the lungs, followed by a decline. The comet assay can detect alkaline sensitive sites, in which DNA adducts are formed (Tice et al., 2000); therefore, the results of our comet assay, in which the highest genotoxic activity who observed at 24 h after injection, could correspond to the data of DNA adduct formation by 1,6-DNP.

It is well known that the metabolites of nitro-PAHs by cellular enzymes bind to DNA to form DNA adducts. Nitro-PAHs form *N*-hydoroxylamines by nitroreduction, followed by activation by *O*-esterification (Arlt et al., 2003). In human, these metabolisms are mediated by phase II enzymes such as *N*-acetyltransferase and sulfotransferase and so on (Arlt et al., 2003). Moreover, the DNA adducts derived from nitro-PAH can induce gene mutation associated with carcinogenesis (Ritter et al., 2002). 3,6-DNBeP might be activated by those enzymes in a similar manner, however, the mechanisms of genotoxicity of 3,6-DNBeP are still unclear. Therefore, further studies regarding the mechanisms of genotoxicity of 3,6-DNBeP are necessary.

In conclusion, several epidemiological studies have demonstrated that environmental air pollution has a tendency to be associated with the incidence of lung cancer and cardiopulmonary mortality (Pope et al., 2002; 2004). Therefore, it is important to monitor such compounds in our environment and evaluate their effects on human health. We demonstrated that 3,6-DNBeP was genotoxic in *in vivo* assay systems. Moreover, 3,6-DNBeP showed equivalent or further genotoxic activity when compared with other nitro-PAHs such as DNP isomers. DNP isomers show carcinogenicity in experimental animals and are thought to be human carcinogens in the environment. Thus, 3,6-DNBeP could be carcinogenic in experimental animals and also in humans. Further studies on genotoxicity mechanisms including DNA adduct formation, carcinogenicity, and exposure levels of 3,6-DNBeP should be conducted.

We thank Dr. Takamichi Ichinose for technical supports.

REFERENCES

Arashidani K, Someya T, Yoshikawa M, Kodama Y. 1992. Polynuclear aromatic hydrocarbon concentration and mutagenic activity in soils sampled at the roadsides. J Jpn Soc Air Pollut 27:190–197.

Arlt VM, Sorg BL, Osborne M, Hewer A, Seidel A, Schmeiser HH, Phillips DH. 2003. DNA adduct formation by the ubiquitous environmental pollutant 3-nitrobenzanthrone and its metabolites in rats. Biochem Biophys Res Commun 300:107–114.

Brown KW, Donnelly , Thomas JC, Davol P, Scott BR. 1985. Mutagenicity of three agricultural soils. Sci Total Environ 41:173–186.

Gibson TL. 1983. Sources of direct-acting nitroarene mutagens in airborne particulate matter. Mutat Res 122:115–121.

Hasei T, Watanabe T, Hirayama T. 2006. Determination of 3, 6-dinitrobenzo[*e*]pyrene in surface soil and airborne particles by high-performance liquid chromatography with fluorescence detection. J Chromatogr A 1135:65–70.

Hayashi M, Tice RR, MacGregor JT, Anderson D, Blakey DH, Kirsh-Volders M, Oleson FB Jr, Pacchierotti F, Romagna F, Shimada H. 1994. In vivo rodent erythrocyte micronucleus assay. Mutat Res 312:293–304.

International Agency for Research on Cancer. 1989. IARC Monographs on the evaluation of carcinogenic risks of chemicals to humans, Vol. 46,Diesel and gasoline engine exhausts and some nitroarenes, IARC, Lyons, France.

International Agency for Research on Cancer. 1996. IARC Monographs on the evaluation of carcinogenic risks of chemicals to humans, vol. 65,Printing processes and printing inks, carbon black and some nitro compounds, IARC, Lyons, France.

Kawanishi M, Watanabe T, Hagio S, Ogo S, Shimohara C, Jouchi R, Takayama S, Hasei T, Hirayama T, Oda Y, Yagi T. 2009. Genotoxicity of 3, 6-dinitrobenzo[*e*]pyrene, a novel mutagen in ambient air and surface soil, in mammalian cells *in vitro* and *in vivo*. Mutagenesis 24:279–284.

Knize MG, Takemoto BT, Lewis PR, Felton JS. 1987. The characterization of the mutagenic activity of soil. Mutat Res 192:23–30.

Leiter J, Shimkin MB, Shear MJ. 1942. Production of subcutaneous sarcomas in mice with tars extracted from atmospheric dusts. J Natl Cancer Inst 3:155–165.

Lewtas J, Chuang J, Nishioka M, Petersen B. 1990. Bioassay-directed fractionation of the organic extract of SRM 1649 urban air particulate matter. Int J Environ Anal Chem 39:245–256.

Nagy E, Zeisig M, Kawamura K, Hisamatsu Y, Sugeta A, Adachi S, Möller L. 2005. DNA adduct and tumor formation in rats after intratracheal administration of the urban air pollutant 3-nitrobenzanthrone. Carcinogenesis 26:1821–1828.

Nishimura T, Goto S, Kata Y, Okunuki M, Matsushita H. 1984. Mutagenicity and benzo[*a*]pyrene contents in soils in Tokyo. J Jpn Soc Air Pollut 19:228–238.

O'Donocan MR. 1990. 1, 8-Dinitropyrene: Comparative mutagenicity in Chinese hamster V79 and CHO cells. Mutagenesis 5:275–277.

Otohuji T, Horikawa K, Maeda T, Sano N, Izumi K, Otsuka H, Tokiwa H. 1987. Tumorigenicity test of 1, 3- and 1,8-dinitropyrene in BALB/c mice. J Natl Cancer Inst 79:185–188.

Pope CA III, Burnett RT, Thun MJ, Calle EE, Krewski D, Ito K, Thurston GD. 2002. Lung cancer, cardiopulmonary mortality, and long-term exposure to fine particulate air pollution. J Am Med Assoc 287:1132–1141.

Pope CA III, Burnett RT, Thurston GD, Thun MJ, Calle EE, Krewski D, Goldleski JJ. 2004. Cardiovascular mortality and long-term exposure to particulate air pollution, epidemiological evidence of general pathophysiological pathways of disease. Circulation 109:71–77.

Ritter LC, Culp JS, Freeman PJ, Marques MM, Beland AF, Malejka-Giganti D. 2002. DNA adducts from nitroreduction of 2, 7-dinitrofluorene, a mammary gland carcinogen, catalyzed by rat liver or mammary gland cytosol. Chem Res Toxicol 15:536–544.